



Density Functional Theory studies of structural, electronic and optical properties of Fluorine Doped Magnesium Hydride


Bello Mustapha^{1,2*}, Abdullahi Lawal³⁺, Aliyu Mohammed Aliyu¹, and Saddiq Abubakar Dalhatu¹

¹Department of Physics, Faculty of Science, Bauchi State University Gadau, Bauchi State, Nigeria.

²Department of Physics, Federal College of Education (Technical) Omoku, Rivers State Nigeria.

³Department of Physics, Federal College of Education Zaria, P.M.B 1041, Zaria, Kaduna State Nigeria.

*Correspondence: [*mustaphabelloazare@gmail.com](mailto:mustaphabelloazare@gmail.com); [+abdullahikubau@yahoo.com](mailto:abdullahikubau@yahoo.com)

Abstract	Article History
<p>In order to overcome the disadvantages of magnesium hydride (MgH₂) towards its applications in solar cell science and technology, doping with non-metals such as Fluorine (F) doping is a promising approach to tune its large band gap. In order to expose the hidden potential in F doped MgH₂, details analysis of electronic and optical absorptions is needed. Theoretical calculations of structural, electronic and optical properties of F doped MgH₂ are studied using first-principles approach within density functional theory (DFT) framework. The calculated lattice constants with PBE-GGA are in better agreement with experimental result. The bandgap value of 3.34 eV for the undoped MgH₂ is close to experimental value. When one atom of F is introduced into MgH₂ at Mg site, the doping effects modified the band gap from 3.34 to 2.72 eV. Also, by introducing one atom of F to H site, the band gap value reduced to 1.59 eV. Our findings confirmed that non-metal doping narrow the energy band gap of semiconductor materials. The results of optical absorptions indicate that F doped MgH₂ at H has strong absorption behavior in the visible light frequency, which depicts its suitability for solar cell applications.</p>	<p>Received: 09/09/2022 Accepted: 20/09/2022 Published: 10/10/2022</p>
<p>How to cite this paper: Mustapha, B., Lawal, A., Aliyu, A.M., and Dalhatu, S.A. (2022). Density Functional Theory studies of structural, electronic and optical properties of Fluorine Doped Magnesium Hydride. <i>Gadau J Pure Alli Sci</i>, 1(2): 145-152. https://doi.org/10.54117/gjpas.v1i2.35.</p>	<p>Keywords DFT; MgH₂; Fluorine; Doping; Solar cell</p> <p>License: CC BY 4.0*</p>  <p>Open Access Article</p>

1.0 Introduction

Solar energy is the most reliable renewable energy source (Li *et al.*, 2022). Apparently, the sunlight supplies approximately 10⁴ times larger energy than our present needs (Radzwan *et al.*, 2018). However, the biggest challenge is the conversion of solar energy into electrical through cheaper technology. In order to resolve this issue, photovoltaic (PV) technology is the most practical and attractive approach to exploit the sustainable energy. Although semiconductor materials are already exploited in the technology, most of the solar panels are dominated by crystalline silicon (Si) technology. However, there are some disadvantages of using silicon for solar cells such as high cost because its fabrication and extraction from raw materials need sufficient efforts (Sopian *et al.*, 2017). The dire requirements for a more efficient, low-cost, and non-

toxic optoelectronic devices has led to the increased focus on a range of different source materials along with the development of methodologies to characterize these materials. In this regards, Magnesium Hydride (MgH₂) is considered a promising candidate owing to its abundance, less-toxicity and low cost (Varunaa *et al.*, 2019). Large band gap of MgH₂ for about 5.16 eV has limited its application for solar cells device (Bahou *et al.*, 2020; Isidorsson *et al.*, 2003; Krasko, 1982). To use MgH₂ as photoactive material for solar cell application, the bandgap value must be tuned. Nowadays, doping is one of the well-developed processes to modify the physical properties of materials. Doping can dramatically modify physical and chemical properties of materials (Jiang *et al.*, 2021). Conversely, non-metal doping is an approach used to narrow the bandgap; in comparison to metal

doping that often forms a donor level in the forbidden band, non-metal doping usually shifts the valence band edge upward (Reisner and Pradeep, 2014). Doping with non-metal elements such as fluorine (F) shows an enhancement in the electronic, optical, and magnetic properties of semiconductor material (Liu *et al.*, 2020; Ren *et al.*, 2008; Wu *et al.*, 2021). The above-mentioned reasons motivated us to study the doping by fluorine atom, which can significantly modify/tune the electronic and optical properties of MgH₂. To the best of our knowledge, no studies on F-doped MgH₂ exist in literature. The F doping approach in MgH₂ may open new paths to non-metal elements doping for various other potential applications such as infrared detectors, infrared LEDs, lasers, transistors, and thermo-photovoltaic systems. Therefore, the main objectives of this paper are to analyze the optoelectronic properties of F doped MgH₂ for solar cell application. First-principles calculations within the framework of density functional theory (DFT) is the method of choice for investigating material properties at the ground state. This method was proposed by famous Hohenberg and Kohn in 1964 as an approach to determine the electronic structure of a system at the ground state. DFT in principle provides an exact description of material physical properties at ground states although approximations become necessary. In this work, structural and electronic properties calculations are performed within DFT framework as implemented in Quantum Espresso simulation package (Giannozzi *et al.*, 2009). Optical properties are calculated using many-body perturbation theory (MBPT) as implemented in Yambo package.

2.0 Materials and methods

In this paper, a well-established tool that does not rely on any fitting techniques or special model called DFT approach is used throughout. The structural and electronic properties of F doped MgH₂ were calculated within DFT framework. For full first-principles philosophy, all calculations have been performed with fully optimized lattice parameters. The first-principles DFT calculations were carried out using pseudopotential method with plane-wave as a basis set. The calculations were performed within the Quantum-Espresso package. Plane-wave kinetic energy cut-offs were set at 50 Ry. The Brillouin zone was sampled with a 10×10×10 Monkhorst-Pack grid of k-points. The geometry relaxation calculations were performed using PBE-GGA. Moreover, to correct the underestimated electronic band gap obtained from DFT calculations, starting from DFT eigen functions and eigenvalues which are solution of Eq.1 to obtain a real quasiparticle (QP) energy E_{nk}^{QP} correction to the Kohn-Sham eigenvalues E_{nk}^{DFT} as in Eq.2 (Idris *et al.*, 2021).

$$\varphi_{nk}^{DFT} E_{nk}^{DFT} = (T + V_H + V_{ne} + V_{XC}) \varphi_{nk}^{DFT} \quad (1)$$

$$E_{nk}^{QP} = Z_{nk} \langle \varphi_{nk}^{DFT} | \Sigma_{GW}(E_{nk}^{DFT}) - V_{XC} | \varphi_{nk}^{DFT} \rangle + E_{nk}^{DFT} \quad (2)$$

where T is the kinetic energy operator, V_H is the Hartree potential, V_{ne} is the potential of the nuclei, V_{XC} is the DFT exchange-correlation potentials and k and n are the k-point and band indices respectively, Σ_{GW} is the GW self-energy which is the product of one-electron Green's function, G and screened Coulomb potential, W as iG_0W_0 , E_{nk}^{DFT} and φ_{nk}^{DFT} are the KS eigen functions and Z_n is the orbital renormalization factor which is defined as shown in Eq. 3 (Lawal *et al.*, 2022)

$$Z_{nk} = \left[1 - \frac{\partial \langle \varphi_{nk}^{DFT} | \Sigma_{GW}(E_{nk}^{DFT}) | \varphi_{nk}^{DFT} \rangle}{\partial E_{nk}^{DFT}} \right]^{-1} \quad (3)$$

3.0 Results and discussions

3.1 Convergence test of E_{cut} and k-point

Performing convergence test calculation before structural, electronic and optical properties calculation is a basic requirement for first-principles calculations within the framework of DFT. The result presented in Figure 1(a) is the obtained convergence tests with respect to the plane wave kinetics energy cut-off and k-points mesh. The converging test in Figure 1(a) illustrated that the total energy varies substantially with respect to the kinetic energy cut-off 10 Ry to 30 Ry and remains almost constant at 40 Ry. As such, 50 Ry is taken as the value for the kinetic energy cut-off for all our calculations. The variations of the total energy with k-points are presented in Figure 1(b). Nevertheless, the total energy changes substantially with the number of k-points, signifying a well-converged value at exact point. However, the total energy increases from $4 \times 4 \times 4$ to $8 \times 8 \times 8$ k-point grids and remain almost steady at $8 \times 8 \times 8$ k-points. Therefore, $10 \times 10 \times 10$ k-point was used for all our calculations.

3.2 Structural properties of MgH₂

In order to find the equilibrium structural ground state properties of the MgH₂ compound, such as the lattice constants, the structure relaxation via Quantum Espresso code using different exchange potentials. Initially, the experimental lattice parameters of the MgH₂ compound were used for the structural optimization process. The geometric parameters of MgH₂ are shown in Table 1. The calculated total energies are fitted to the Murnaghan's equation (Tyuterev and Vast, 2006) of state to determine the ground state properties. The calculated lattice parameters with different exchange correlation potentials together with experimental result are listed

in Table 1. It is seen that the lattice constants obtained with PBE-GGA are in better agreement with experimental data. PBEsol-GGA gives out more errors among the exchange functionals used and the largest portion of error is coming from c while LDA underestimate lattice parameters.

3.3 Electronic properties

Electronic properties calculation is important due to interpretation of electronic properties of solids (Radzwan *et al.*, 2020). The investigation of electronic properties of pure MgH_2 and F doped MgH_2 comprises of band structure, density of state (DOS) and partial density of state (PDOS). Fluorine was added to pure at H and Mg sites in the calculations in order to understand the effect of doping. The calculated electronic band structure for both undoped and F doped MgH_2 are shown along the high symmetry point Γ -X-M- Γ -Z-A-R-Z-W of the first Brillouin zone (BZ). The Fermi level is indicated by the zero-energy scale on the band structure. A generalised gradient approximation (PBE-GGA) was preferred over Local Density Approximations (LDA) due to its reliability and accuracy in DFT calculations (Lawal *et al.*, 2017b; Radzwan *et al.*, 2020). The energy separation between the conduction band minimum (CBM) and the valence band maximum (VBM) occurred at X and Z points which indicates an indirect band gap material with

value of 3.34 eV energy band gap and this value corresponds to the energy band gap of pure MgH_2 . The calculated band gap of pure MgH_2 is close to experimental value when compared with previous first principle calculations of value 2.01 eV (Irfan and Azam, 2020). Consistency of our results with experimental value is due to convergence test of energy cut-off, k-point and structural relaxation of the lattice parameters. It can be observed that the energy band gap reduces considerably by doping F at Mg and H atoms sites as can be seen in Figure 3(b) and 3(c). The bandgap of single-atom F doped MgH_2 at Mg site is reduced from 3.34 to 2.72 eV. For F doped MgH_2 at H site the band gap value reduced to 1.59 eV. This trend of reduction of band gap value for none-metal doping on large band gap material is in good agreement with previous theoretical approach (Butt *et al.*, 2018; Lawal *et al.*, 2021; Radzwan *et al.*, 2020) and experiment measurement (Mushtaq *et al.*, 2016). The electronic band gap values calculated in this paper together with previous first-principles and experimental results are tabulated in Table 2. From our findings, the material that can be used for solar cell application is the one in which F is doped at H site of MgH_2 , because its band gap is within the visible light wavelengths.

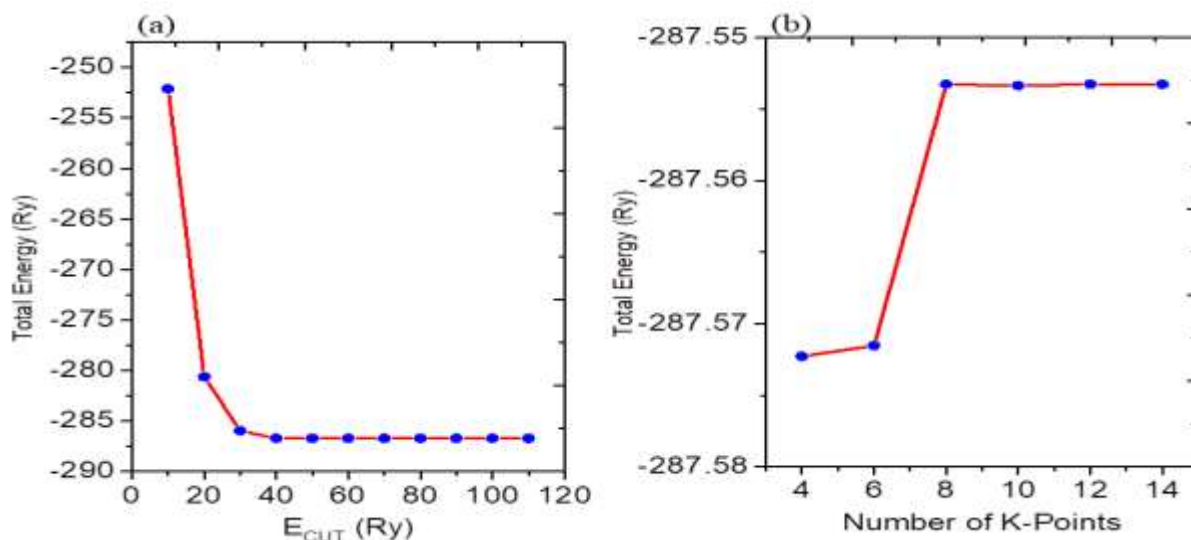


Figure 1: (a) The convergence of total energy with respect to the kinetic energy cut-off. (b) The convergence of the total energy with respect to the k-points grids.

Table 1: Calculated and experimental lattice constants of MgH_2

Reference	XC	a (Å)	b (Å)	c (Å)
Present work	LDA	4.252	4.252	2.884
	PBE-GGA	4.540	4.540	2.994
	PBEsol-GGA	4.631	4.631	3.340
	GGA-WC	4.562	4.562	3.162
Experiment (Bortz <i>et al.</i> , 1999)		4.501	4.501	3.010

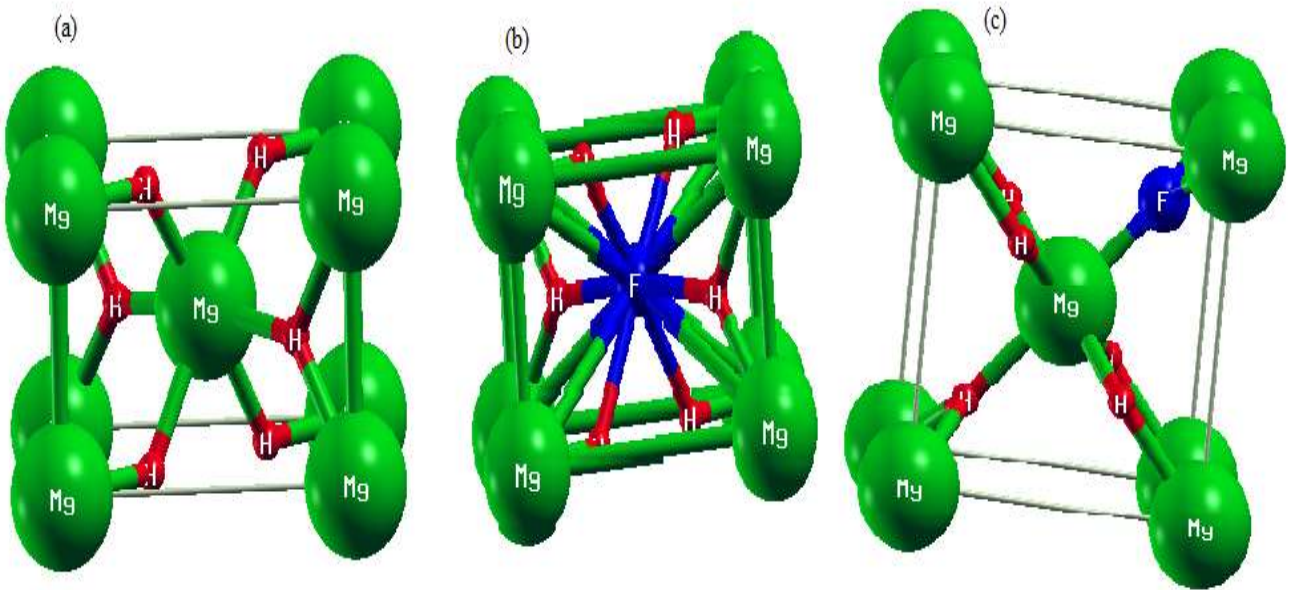


Figure 2: Schematic diagram of crystal structure of (a) Pure MgH_2 (b) F doped MgH_2 at Mg site (c) F doped MgH_2 at H site

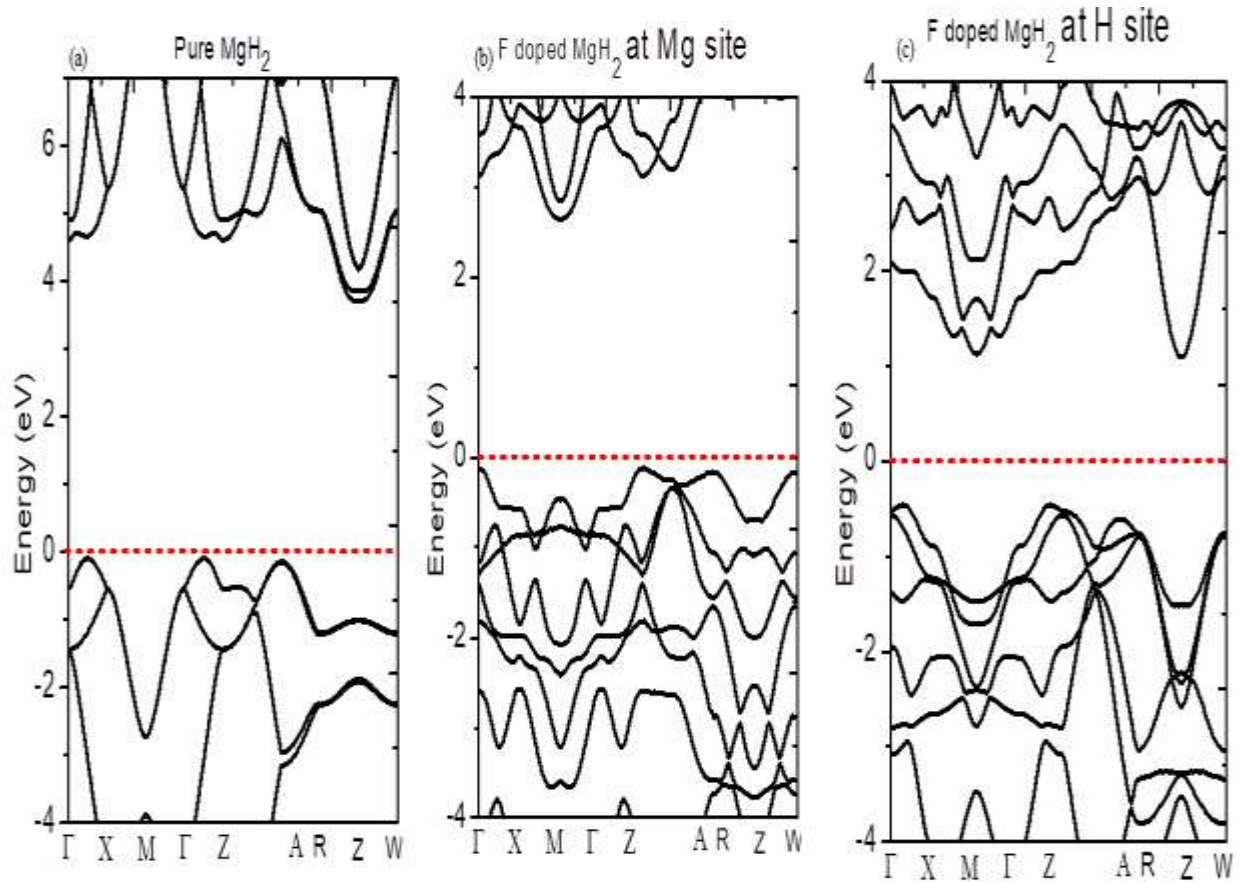


Figure 3: Band structure of (a) Pure MgH_2 (b) F doped MgH_2 at Mg site and (c) F doped MgH_2 at H site

Table 2: Calculated band gap values of pure MgH₂ and F doped MgH₂ together with available experimental data and other first principles calculations

Polymorph	Methods	Bandgap value, E _g (eV)
MgH ₂	PBE-GGA	3.34
	PBE-GGA (Irfan and Azam, 2020)	2.01
F doped MgH ₂ at Mg site	PBE-GGA	3.06
	PBE-GGA	2.72
Fdoped MgH ₂ at H site	PBE-GGA	1.59

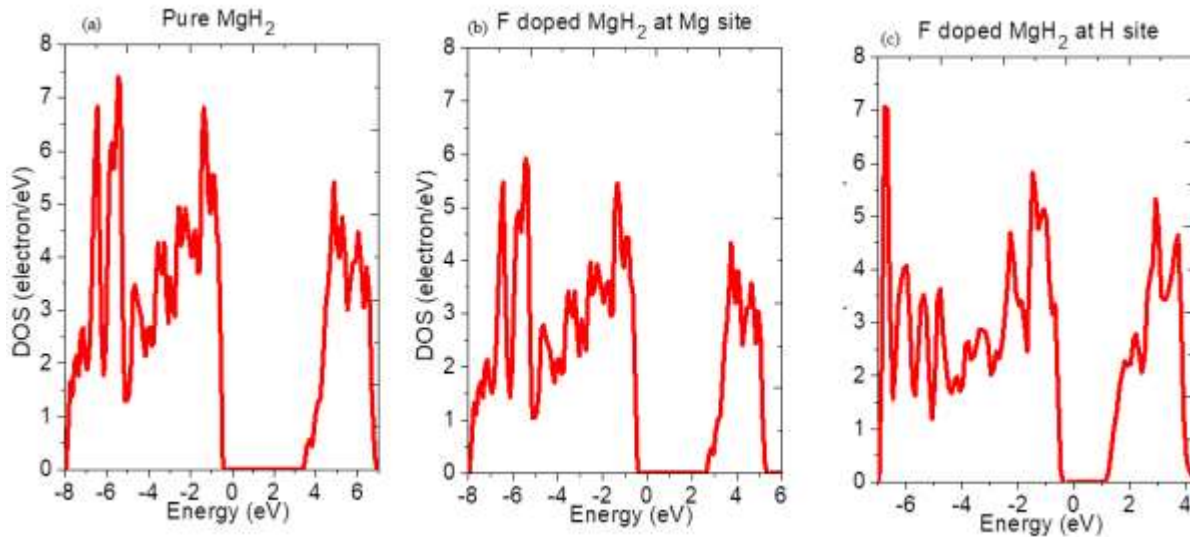


Figure 4: Total density of states (DOS) of (a) Pure MgH₂ (b) F doped MgH₂ at Mg site (c) F doped MgH₂ at H site

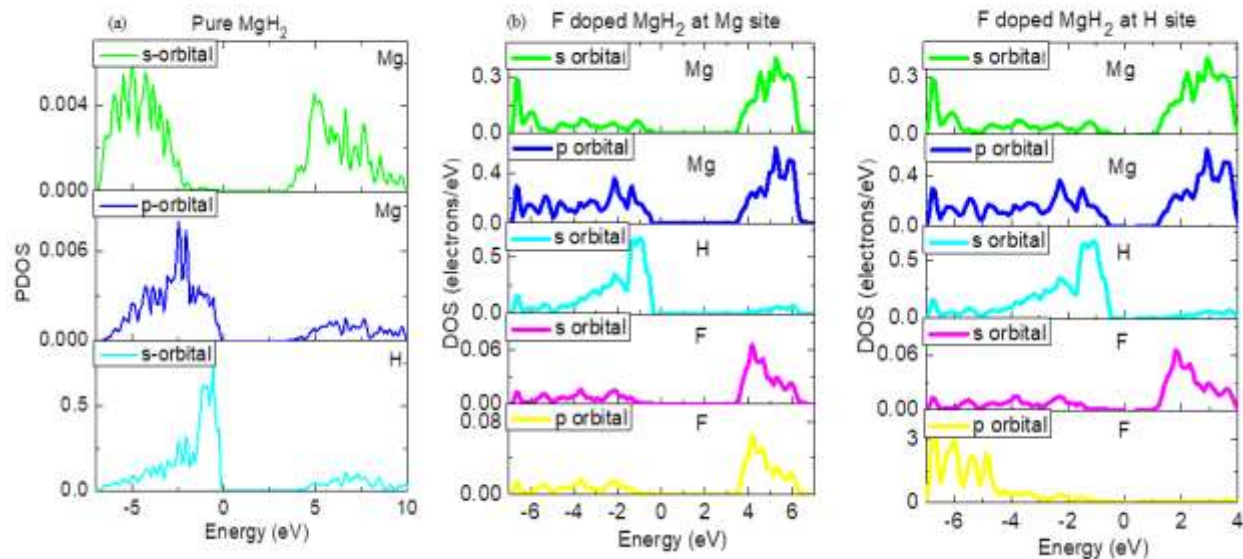


Figure 5: Partial density of states (DOS) of (a) Pure MgH₂ (b) F doped MgH₂ at Mg site (c) F doped MgH₂ at H site

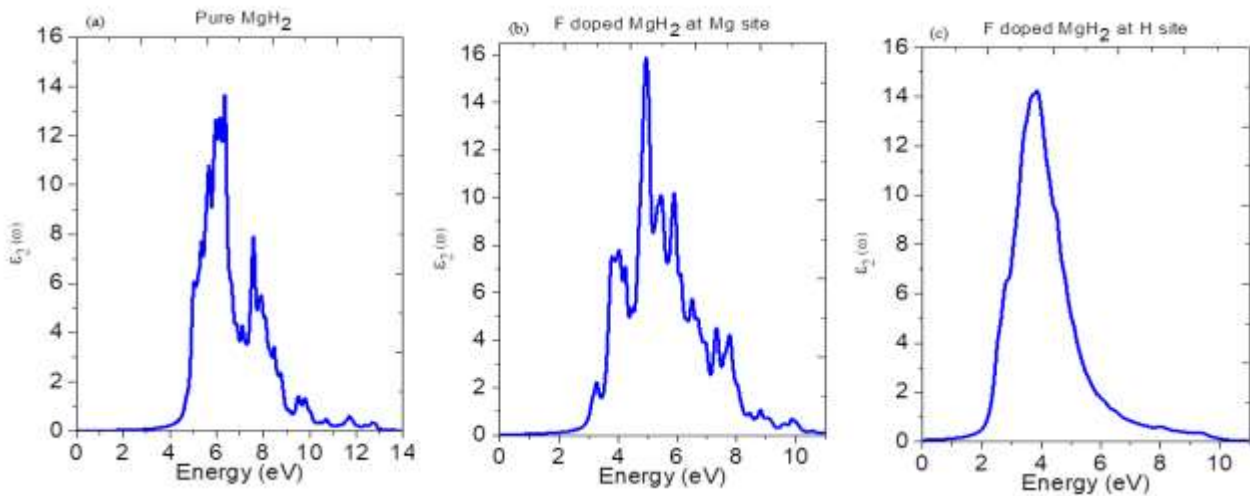


Figure 6: The imaginary part of frequency-dependent dielectric function of: (a) Pure MgH₂ (b) F doped MgH₂ at Mg site and (c) F doped MgH₂ at H site

Total density of state (DOS) and partial density of state (PDOS) were studied in order to understand the nature of energy gap clearly. Figures 4 and 5 show DOS and PDOS results respectively, both Figures illustrated higher peaks at the valence bands and lower peaks at the conduction bands. In the case of pure MgH₂, the lowest valence states are dominated by *s*-, *p*-orbital of Mg atoms and *s*-orbital of H atom. The *s*-orbital of Mg atoms have the highest contribution in the conduction band with little contributions of *p*-orbital of Mg and *s*-orbital of H atoms. Figure 5 depicts the PDOS of F doped MgH₂ at Mg site, *p*. The energetically conduction bands are principally due to *s*- and *p*-orbitals of Mg and F atoms. The upper valence bands near the Fermi level is due to *s*-orbitals of H atoms. For F doped MgH₂ at H site, the lowest of the conduction bands consists of *s*-orbitals of Mg and H atoms together with *p*-orbital of Mg atoms. The maximum of the valence band near to the Fermi level comes from *s*-orbitals of H while the core of valence bands is due to *p*-orbital of F atoms.

3.4 Optical properties of pure and F-doped MgH₂

The study of optical properties due to electronic transition is related to electronic properties (Lawal *et al.*, 2022). The ability to capture, transmit and efficiently transform the photons into electricity is one of the interesting characteristics of the optoelectronic properties of materials (Lawal *et al.*, 2019). Hence, the knowledge of the optical properties of the F-doped MgH₂ is considered a key in realizing the dream of its practical application besides electronic properties. In the optical approach, excited states is represented as unoccupied Kohn-Sham states. Transitions between occupied and unoccupied states are caused by the electric field of the photon. When the excitations are collective, they are known as plasmons (which are most easily observed by the passing of a fast electron through the system rather than a photon). When the

transitions are independent, they are known as single particle excitations (Lawal *et al.*, 2017b). The spectra resulting from these excitations can be thought of as a joint density of states between the valence and conduction bands. This part provides information as regards to optical absorptions of undoped and doped MgH₂ which was examined for the first time by highly accurate first principles pseudopotential plane wave method as implemented in Yambo code. Optical absorption of material normally explains the behavior of material when exposed to the electromagnetic radiation and it also helps in predicting band structure configuration. Optical behavior is strongly associated with electronic band structure (Cohen and Chelikowsky, 2012; Ni *et al.*, 2021). Several experimental studies showed that optical properties of doped materials depended on the concentration of dopant element. However, to the best of our knowledge, theoretical investigation on F doped MgH₂ have not been reported yet. In order to describe the said parameter quantitatively, it is essential to evaluate frequency dependent dielectric function $\epsilon(\omega)$. Dielectric function is the ratio of the permittivity of a material to the permittivity of free space, whereas permittivity is the measure of the resistance of a material when an electric field is induced in a material. All dielectric materials are insulators but all insulators are not dielectric (Subramanian *et al.*, 2000). The dielectric function consists of real $\epsilon_1(\omega)$ and imaginary part $\epsilon_2(\omega)$. It is represented as follows:

$$\epsilon(\omega) = \epsilon_1(\omega) + i\epsilon_2(\omega) \quad (4)$$

where $\epsilon_1(\omega)$ is real part and $\epsilon_2(\omega)$ is imaginary part of the dielectric function. Physical properties and band structure rely strongly on $\epsilon(\omega)$.

As mentioned, we analyzed optical absorption based on PBE-GGA functional. From the knowledge of electronic band structure of a solid, the imaginary part of the dielectric function, $\epsilon_2(\omega)$ can be calculated from

Kubo–Greenwood equation as show in Equation 2 (Lawal *et al.*, 2017a):

$$\varepsilon_2(\omega) = \frac{2\pi e^2}{\Omega \varepsilon_0} |\langle \psi_k^c | \hat{u} \times \vec{r} | \psi_k^v \rangle| \delta(E_k^c - (E_k^v + E)) \quad (5)$$

The calculated imaginary (ε_2) parts of the dielectric functions as a function of the photon energy for undoped and F doped Mg are shown in Figure 6.

The edge of optical absorption (first critical point) occurs at about 3.34, 2.72 and 1.59 eV for pure MgH₂, F doped MgH₂ at Mg site and F doped at H respectively. Hence, the calculated imaginary part of dielectric function shows that the first critical point peak is related to the transition from the valence to the conduction band states which corresponds to the fundamental band gap. The results of imaginary part of dielectric function indicate that F doped MgH₂ at H has strong absorption behavior in the visible light frequency, which depicts its suitability for solar cell applications. In the imaginary part of the dielectric function, F doped MgH₂ at Mg and H sites are found to be zero at higher energy of >10eV, which shows that the structures have achieved the equilibrium value of zero. This suggests that the functionalities of F doped MgH₂ is limited under ultraviolet range, which is in consistent with the role as a photovoltaic (PV) material. However, the obtained spectrum still covers a wide energy range that is not restricted only to the visible region. In PV applications, high potential materials rendering high absorption intensity are used as an absorbing medium of the electromagnetic radiation. From the spectra comparison, F doped MgH₂ depicts better absorption quality than pure MgH₂. The response of each structure is also different in terms of the energy absorbing radiations. The absorption spectrum of F doped MgH₂ at H site shows better capability in absorbing the radiation at low frequency than pure MgH₂ and F doped MgH₂ at Mg site as electromagnetic radiation of the 1.59 eV energy can be easily absorbed.

4.0 Conclusion

In this paper, structural, electronic and optical properties of pure MgH₂ and F doped MgH₂ were studied using DFT formalism. It is seen that the lattice constants obtained with PBE-GGA are in better agreement with experimental data when compared with other exchange potentials. Our band structure results revealed that the material that can be used for solar cell application is the one in which F is doped at H site of MgH₂, because its band gap of 1.59 eV is within the visible light wavelengths. Based on this, it can be concluded that the results of this research work confirmed the decreasing of band gap when non-metal is added to material with wider energy band gap. The results of optical spectra indicate that F doped MgH₂ at H has strong absorption behaviour in the visible

light frequency, which depicts its suitability for solar cell applications. Our theoretical study of F-doped MgH₂ suggests that a device fabricated from these materials can be operated on a wide range of the energy scale such as solar cell and broadband photodetector.

Declarations

Ethics approval and consent to participate

Not Applicable

Consent for publication

All authors have read and consented to the submission of the manuscript.

Availability of data and material

Not Applicable.

Competing interests

All authors declare no competing interests.

Funding

There was no funding for the current report.

References

- Bahou, S., Labrim, H., Lakhal, M., Bhihi, M., Hartiti, B., and Ez-Zahraouy, H. (2020). Improving desorption temperature and kinetic properties in MgH₂ by vacancy defects: DFT study. *international journal of hydrogen energy*, 45(18), 10806-10813.
- Bortz, M., Bertheville, B., Böttger, G., and Yvon, K. (1999). Structure of the high pressure phase γ -MgH₂ by neutron powder diffraction. *Journal of Alloys and Compounds*, 287(1-2), L4-L6.
- Butt, F. K., Li, C., Haq, B. U., Tariq, Z., and Aleem, F. (2018). First-principles calculations of nitrogen-doped antimony triselenide: A prospective material for solar cells and infrared optoelectronic devices. *Frontiers of Physics*, 13(3), 137805.
- Cohen, M. L., and Chelikowsky, J. R. (2012). *Electronic structure and optical properties of semiconductors* (Vol. 75): Springer Science and Business Media.
- Giannozzi, P., Baroni, S., Bonini, N., Calandra, M., Car, R., Cavazzoni, C., . . . Dabo, I. (2009). QUANTUM ESPRESSO: a modular and open-source software project for quantum simulations of materials. *Journal of physics: Condensed matter*, 21(39), 395502.
- Idris, B., Lawal, A., Abubakar, D., and Dalhatu, S. A. (2021). Ab initio Calculation of CuSbSe₂ in Bulk and Monolayer for Solar Cell and Infrared Optoelectronic Applications. *Communication in Physical Sciences*, 7(3).
- Irfan, M., and Azam, S. (2020). *Structural, Electronic and Optical Properties of MgH₂, CaH₂ for Hydrogen Storage Materials: First principles study* (2516-2314). Retrieved from

- Isidorsson, J., Giebels, I., Arwin, H., and Griessen, R. (2003). Optical properties of MgH₂ measured in situ by ellipsometry and spectrophotometry. *Physical Review B*, 68(11), 115112.
- Jiang, Y., Du, M., Cheng, G., Gao, P., Dong, T., Zhou, J., . . . Dai, L. (2021). Nanostructured N-doped carbon materials derived from expandable biomass with superior electrocatalytic performance towards V²⁺/V³⁺ redox reaction for vanadium redox flow battery. *Journal of Energy Chemistry*, 59, 706-714.
- Krasko, G. (1982). Electronic Properties and Equilibrium Lattice Parameters of Magnesium Hydride. In *Metal-Hydrogen Systems* (pp. 367-380): Elsevier.
- Lawal, A., Bello, M., and Kona, A. M. (2022). Quasi-particle band structure and optical properties of Perylene Crystal for Solar Cell Application: A G₀W₀ Calculations. *Communication in Physical Sciences*, 8(2).
- Lawal, A., Shaari, A., Ahmed, R., and Jarkoni, N. (2017a). First-principles investigations of electron-hole inclusion effects on optoelectronic properties of Bi₂Te₃, a topological insulator for broadband photodetector. *Physica B: Condensed Matter*, 520, 69-75.
- Lawal, A., Shaari, A., Ahmed, R., and Jarkoni, N. (2017b). Sb₂Te₃ crystal a potential absorber material for broadband photodetector: A first-principles study. *Results in physics*, 7, 2302-2310.
- Lawal, A., Shaari, A., Ahmed, R., Taura, L., Madugu, L., and Idris, M. (2019). Sb₂Te₃/graphene heterostructure for broadband photodetector: A first-principles calculation at the level of Cooper's exchange functionals. *Optik*, 177, 83-92.
- Lawal, A., Shaari, A., Taura, L., Radzwan, A., Idris, M., and Madugu, M. (2021). G₀W₀ plus BSE calculations of quasiparticle band structure and optical properties of nitrogen-doped antimony trisulfide for near infrared optoelectronic and solar cells application. *Materials Science in Semiconductor Processing*, 124, 105592.
- Lawal, A., Taura, L., Abdullahi, Y. Z., Shaari, A., Suleiman, A. B., Gidado, A., and Chiromawa, I. M. (2022). Corrections of band gaps and optical spectra of N-doped Sb₂Se₃ from G₀W₀ and BSE calculations. *Physica B: Condensed Matter*, 414307.
- Li, G., Li, M., Taylor, R., Hao, Y., Besagni, G., and Markides, C. (2022). Solar energy utilisation: Current status and roll-out potential. *Applied Thermal Engineering*, 209, 118285.
- Liu, Y., Li, Q., Guo, X., Kong, X., Ke, J., Chi, M., . . . Zeng, J. (2020). A Highly Efficient Metal-Free Electrocatalyst of F-Doped Porous Carbon toward N₂ Electroreduction. *Advanced Materials*, 32(24), 1907690.
- Mushtaq, S., Ismail, B., Raheel, M., and Zeb, A. (2016). Nickel antimony sulphide thin films for solar cell application: study of optical constants. *Natural Science*, 8(2), 33-40.
- Ni, J., Quintana, M., Jia, F., and Song, S. (2021). Tailoring the electronic and optical properties of layered blue phosphorene/XC (X= Ge, Si) vdW heterostructures by strain engineering. *Physica E: Low-dimensional Systems and Nanostructures*, 127, 114460.
- Radzwan, A., Ahmed, R., Shaari, A., Ng, Y. X., and Lawal, A. (2018). First-principles calculations of the stibnite at the level of modified Becke-Johnson exchange potential. *Chinese journal of physics*, 56(3), 1331-1344.
- Radzwan, A., Lawal, A., Shaari, A., Chiromawa, I. M., Ahams, S. T., and Ahmed, R. (2020). First-principles calculations of structural, electronic, and optical properties for Ni-doped Sb₂S₃. *Computational Condensed Matter*, 24, e00477.
- Reisner, D. E., and Pradeep, T. (2014). *Aquananotechnology: global prospects*: CRC Press.
- Ren, Z.-A., Lu, W., Yang, J., Yi, W., Shen, X.-L., Li, Z.-C., . . . Zhou, F. (2008). Superconductivity at 55 K in iron-based F-doped layered quaternary compound Sm [O_{1-x}F_x] FeAs. *arXiv preprint arXiv:0804.2053*.
- Sopian, K., Cheow, S., and Zaidi, S. (2017). *An overview of crystalline silicon solar cell technology: Past, present, and future*. Paper presented at the AIP Conference Proceedings.
- Subramanian, M., Li, D., Duan, N., Reisner, B., and Sleight, A. (2000). High dielectric constant in ACu₃Ti₄O₁₂ and ACu₃Ti₃FeO₁₂ phases. *Journal of Solid State Chemistry*, 151(2), 323-325.
- Tyuterev, V., and Vast, N. (2006). Murnaghan's equation of state for the electronic ground state energy. *Computational materials science*, 38(2), 350-353.
- Varunaa, R., Kiruthika, S., and Ravindran, P. (2019). *Ti⁴⁺ substituted magnesium hydride as promising material for hydrogen storage and photovoltaic applications*. Paper presented at the AIP Conference Proceedings.
- Wu, Y.-b., Li, Y., Zhao, Y.-j., Zhou, W., and Zhong, F.-x. (2021). Preparation and photoelectric properties of F-doped cuprous oxide thin films. *Optical Materials*, 111, 110167.